Cement & Concrete Composites 22 (2000) 39–46

Cement & Concrete Composites

Construction of Benten Viaduct, rigid-frame bridge with seismic isolators at the foot of piers

Minoru Yoshikawa *, Hidenao Hayashi, Shiro Kawakita, Mitsuhiro Hayashida

Hanshin Expressway Public Corporation, 4-1-3 Kyutaro-machi, Chuo-ku, Osaka, Japan

Abstract

'Benten Viaduct' is one of the reconstructed bridges of Hanshin Expressway Route 3, which suffered a significant damage during the Hanshin/Awaji Earthquake in 1995. This section had consisted of 8 bridges before the earthquake, but revived as an innovative structure, 19-span continuous rigid-frame bridge with seismic isolators installed underneath the steel piers. This paper reports the seismic isolation design and construction techniques of this innovative bridge structure, comparing the result of analysis with that of the vibration test using the actual bridge structure.

Keywords: Bridge reconstruction; Hanshin Earthquake; Rigid-frame construction; Seismic isolators; Design; Construction techniques; Testing

1. Introduction

The Hanshin/Awaji Earthquake occurred on 17 January 1995, caused tremendous damage to the Hanshin Expressway Route 3 (Kobe Route), especially at Fukae and Benten sections (see Figs. 1 and 2). The reconstructed bridge, 'Benten Viaduct', was determined to be the 19-span continuous rigid-frame bridge with steel deck along with the installation of seismic isolator. The general view of the structure is shown in Fig. 3.

Before the earthquake, one of the piers stood on the middle of the separating zone and the other on the pedestrian walk, and they were made of single RC pier. These piers were connected with the superstructure by means of steel bearings that were placed on top of each pier. When the earthquake struck, most of the columns collapsed due to shear force, causing the bridge to fail and the girder to buckle. Because they were located above National Highway Route 2 which is also a lifeline route to Kobe City, as much as 24 spans of girders and columns of this section were removed immediately after the earthquake to keep the traffic safety on Route 2. The removal work was completed within 17 days.

2. Design

2.1. Strategy

For restoring the bridges in Benten section, the following three basic strategies were determined:
1. The pile foundations could be utilized as they were since they were found to have no damage.
2. Steel deck and seismic isolation bearings could be used in order to decrease seismic force acting on the foundation.
3. In order to prevent bridges from falling down, each bridge pier and the beam of superstructure would be tied rigidly for the longest possible length.

Based on the strategies above, it was decided to adopt a continuous rigid frame. It was supposed that the additional piling reinforcement would be needed for rigid or hinged connection at the end of the pier. Finally it was concluded to adopt the structure with seismic isolation bearing installed on the foundation (see Table 1). Since the Benten Viaduct is warped to the seaside and the overhang length of cross-beams differs slightly, analysis was made on the entire structural model of the two types shown in Fig. 4.

Both at the east-end and west-end of Benten Viaduct, 2-span continuous steel box girder bridges were arranged as absorber bridges, which were installed so as not to cause a remarkable difference of vibration characteristics from the adjacent existing simple girder bridges.

* Corresponding author.

PII: S0958-9465(99)00047-5

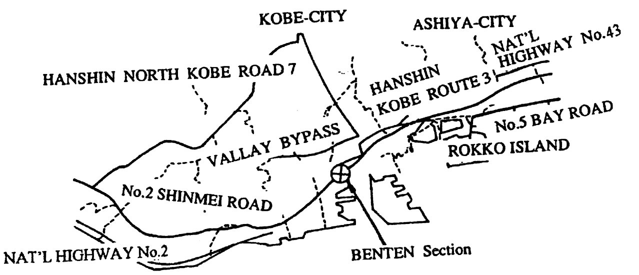

Fig. 1. Location of Benten section.

Fig. 2. Damage at Benten section.

2.2. Outline of design

Model (a) in Fig. 4 was used for static analysis. The superstructure consisted of main girders, beams, and piers which were supported by the two way horizontal spring as well as perpendicular and rotational ones. The characteristic of the isolator is expressed by natural period (T) and the ratio of yield point load (Qd/Wu) [1]. In order to give an appropriate initial coefficient of bearing reaction for the static analysis model, the natural period and the ratio of yield point load were decided using a representative bridge pier that would satisfy the following three design objects:

1. In the designed vibration from the horizontal bearing capacity, piers should not excessively be plastic during the earthquake ($Khe < 0.68$).
2. In the seismic coefficient method, a designed vibration can at least be decreased by the damping effect. (Dumping constant by the seismic coefficient at the vibration $h > 10\%$.)
3. Seismic isolator should not be deformed extremely. (Horizontal bearing capacity during earthquake was investigated referring to the superstructure that deflects < 250%.)

A combination of $T = 1.4$ s and $Qd/Wu = 12.6\%$ has been adopted to satisfy the condition above.

From the static analysis, deflections were calculated for each bearing and for the girders at both ends. Girder's deflection reached ±84 mm maximum depending on the various temperature ranges. Expansion joints were designed based on this movement.

In dynamic analysis, model (b) in Fig. 4 was used. The main girders and deck plates were assembled together to a piece of beam so that they would make an entire simple model. The seismic wave taken at the JR Takatori Station was applied [2] for the input of seismic vibration. Earthquake force of EW wave was put into the chord direction of warped bridge and SN wave to the lateral direction simultaneously.

The time histories were exemplified in Fig. 5 for the response in the horizontal deflection of the seismic isolator and the bending moment at the beam joint at P470. Maximum deflections were 428 mm in the longitudinal direction of the bridge and 568 mm in the transverse direction, which were observed after 6 s of the beginning of earthquake.

The results of natural vibration analysis on the entire model are shown in Fig. 6 and all up to fifth modes show inherent mode of horizontal direction. From the result of natural vibration analysis applied on a plane model, the mode for horizontal move at the bearing position is so remarkable that a similar tendency may be seen in a three-dimensional model.

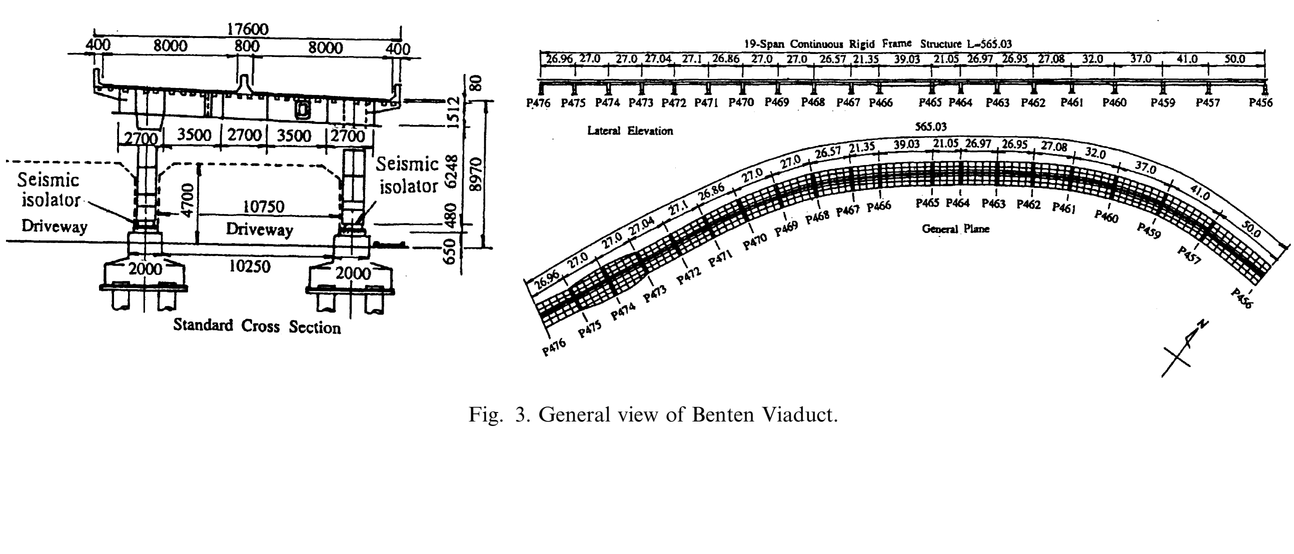

Fig. 3. General view of Benten Viaduct.

Table 1
Comparison of structures

		Rigid connection			Hinge connection			Seismic isolation bearing		
		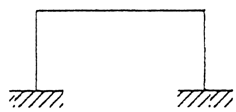			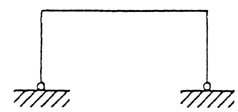			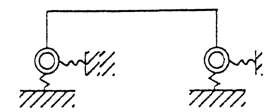		
Column	Stress resultant	V	H	M	V	H	M	V	H	M
	Dead load	227.4	120.4	277.3	227.4	76.9	0.0	227.4	29.3	60.7
	Temperature	227.4	140.1	386.0	227.4	79.6	0.0	227.4	30.6	58.7
	Earthquake	241.2	177.2	531.1	267.9	133.8	0.0	260.1	100.6	10.9
Reaction force on pile		$280 \geqslant 184$ (tf/pile)			$210 \geqslant 184$ (tf/pile)			$175 \leqslant 184$ (tf/pile)		

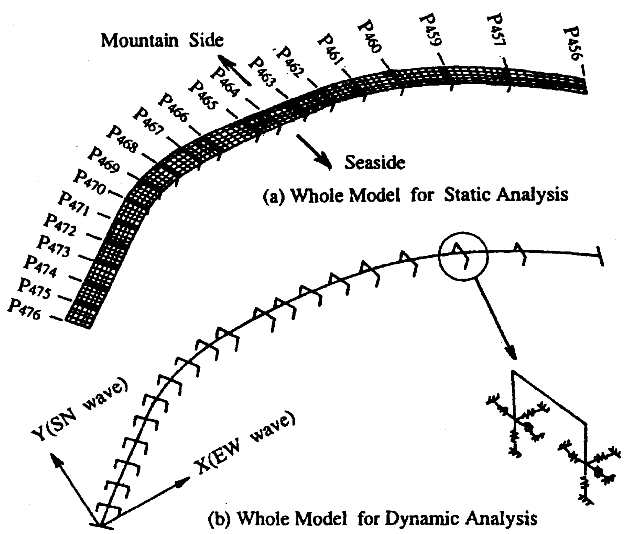

Fig. 4. Entire models for analysis.

Again the stresses at the intersection at the beam and the pier were investigated as members that receive axial compressive force and bi-axial bending moment by applying maximum response values.

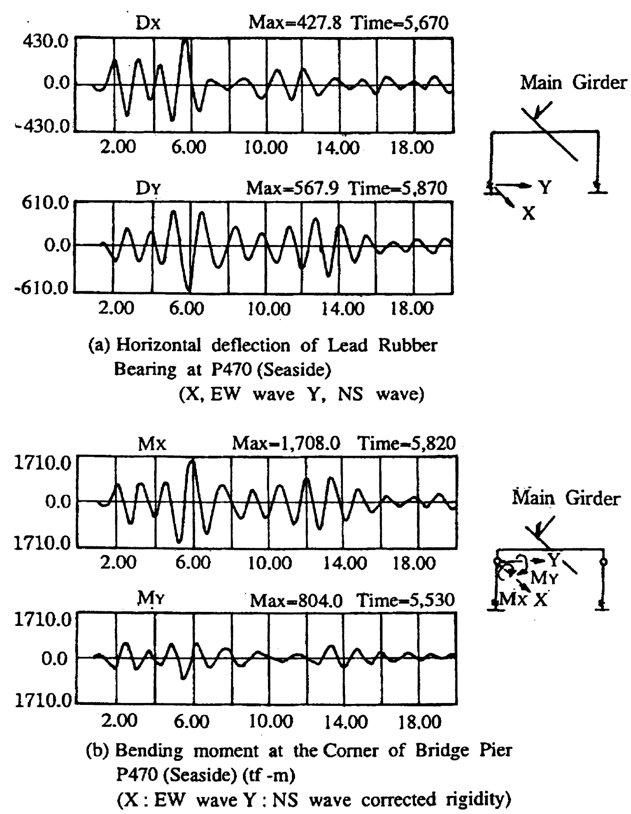

Fig. 5. An example of response analysis on time history.

2.3. Seismic isolator

Seismic isolation bearing was designed referring to the 'Manual of Isolation Design for Highway Bridge'. There are two types of seismic isolators: lead rubber bearing (LRB) and high dumping rubber (HDR). LRB is a laminated-rubber bearing including lead plugs inside to give bi-linear deformation characteristic, while HDR is made of laminated super elastic gum.

Benten Viaduct has so many dimensions statically indeterminate that LRB was adopted because it would be softer on various temperature ranges and harder under strong earthquake force. Each LRB bearing was designed to be of the same height nevertheless the difference of the design supporting load in order to make the deformation characteristics similar. The appearance of seismic isolation bearing is shown in Fig. 7.

Through the static and dynamic analyses, seismic characteristics were corrected as below:

T (natural period of entire superstructure) = 1.45 s,
h (dumping constant of isolator when horizontal displacement = 100 mm) = 22%,
shear deflection of isolator (when $Kh = 0.23$) = 50% (design capacity = 150%),

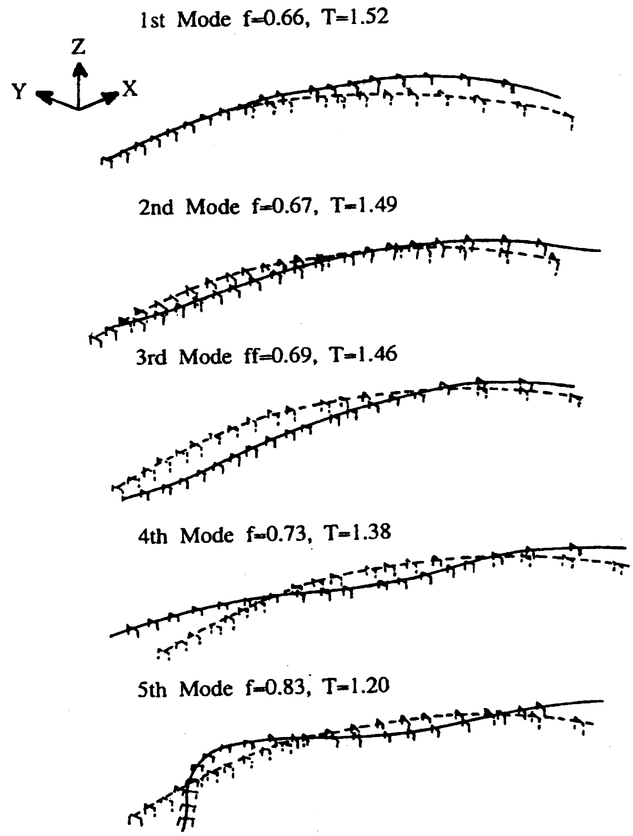

Fig. 6. Results of natural vibration analysis.

Fig. 7. Seismic isolation bearing.

shear deflection of isolator (when $Kh = 0.68$) = 196% (design capacity = 250%),
shear deflection of isolator (dynamic analysis) = 357% (design capacity = 400%).

2.4. Earthquake restrainer

Benten Viaduct is a long continuous rigid-frame bridge which would never fail again. The bridge also has a dumping function against the vibration of earthquakes. Besides, multiple earthquake restrainers were recommended to be placed by the specification [3] of the Ministry of Construction in 1995.

Earthquake restrainers were installed at both ends of the structure where the girders are supported by seismic isolators on ordinary rigid-frame steel piers. They were designed to work for longitudinal direction when the displacement became larger than the limit given by Ductility Design Method. The steel members of the restrainers were designed by Allowable Stress Design Method using a horizontal force as much as vertical bearing capacity.

For transverse direction, side-brick type restrainers were installed on the isolators. They were set 5 mm side away from the upper plate of bearing, and designed with the earthquake force used in Allowable Stress Design Method. This means that the seismic isolator usually restricts its displacement during a smaller earthquake not to break the expansion joint on the road and is expected to show its seismic ability only during a bigger earthquake.

3. Construction work [4]

3.1. Substructure

Before the start of the reconstruction work, bearing capacity (qd) of the ground was investigated using corn penetrating test. Bearing capacity of 300–600 tf/m^2 was observed in most part, however, there was some local area having only 150 tf/m^2 of qd. Foundations on such ground had to be reinforced with adding piles. The number of such foundations was fourteen, which was 30% of all the foundations in Benten section.

As mentioned before, National Highway Route 2 was the only lifeline route to link the east and west part of Kobe, and Benten site was located along the National Highway Route 2. Therefore, the work had to be carried out by closing two lanes night and day out of six lanes.

The location was so close to the downtown and/or the residence area that great deal of attention was paid to reduce vibration or noise from the piling work. The earth drill method and pile jacking with oil hydraulics were adopted regularly.

The reinforcing bars were joined to the existing ones by means of enclosed arc welding. Details of reinforcement of footing are shown in Fig. 8.

3.2. Superstructure

The length of Benten Viaduct is as long as 686 m, which causes ±28 mm expansions at both ends from the

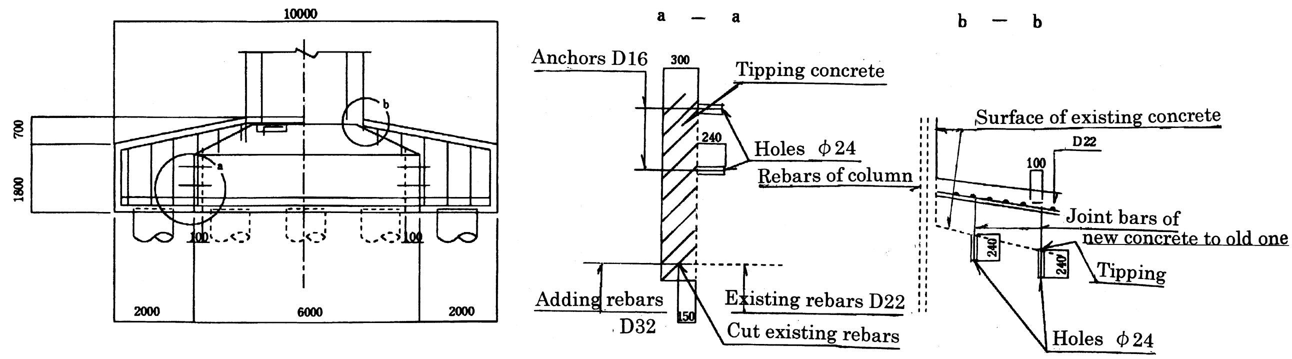

Fig. 8. Reinforcement of footings.

Fig. 9. Erection of main girder.

Fig. 10. State of construction.

difference of temperature of ±10°C. To keep accuracy of erection, columns and cross-beams were built up first. After that, plate girders with steel deck were erected measuring and correcting the errors at each pier point. The deviation of erection was less than 5 mm at every isolators.

Camber for the dead load was solved statically using a partial rigid-frame model. It was found that a horizontal deformation of 3.2–4.7 mm would be caused by the influence of dead load. Since the actual stiffness of each member was supposed to be stronger than the designed one, the influence of camber on the isolators due to the dead load was ignored (see Figs. 9 and 10).

The steel piers were unstable on the soft seismic isolation bearings until they formed a three-dimensional rigid frame. In the practical fieldwork, a stabilizer system was invented as shown in Fig. 11. This system was introduced to stabilize the columns before the erection of girder and deck, and it could also secure the accuracy of piers and bearings. The stabilizer was designed to have a temporary horizontal bearing capacity against 0.15 G.

Fig. 11. Temporary stabilizer system for column.

4. Vibration test [5]

4.1. Outline of experiment

In order to ascertain the dynamic characteristics of the bridge, a series of tests using the actual bridge were

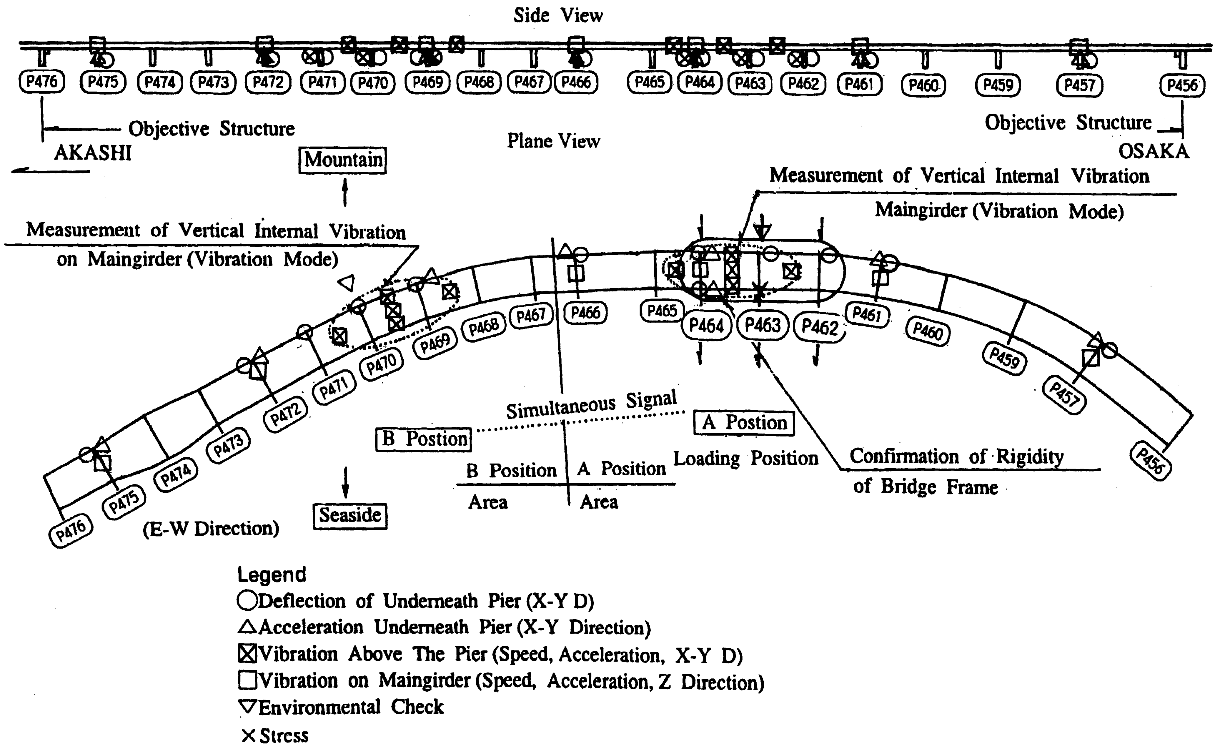

Fig. 12. Loading position and measured position.

carried out. Since the 19-span continuous bridge is so long and heavy, the vibration test by using a vibratory equipment is not feasible. Therefore, a rapid force release test was carried out instead and the free dumping vibration was measured after the release of force. The elastic performance of base isolation was also measured under a static load condition. For grasping vibratory behavior of girders and vibration transmission through seismic isolation, four axles wrecker vehicle of gross weight 47 tf (Maximum four vehicles simultaneously) was used to run on the bridge and response was measured. The reaction force support was installed on the bridge foundation and horizontal force was applied to the lateral direction of the bridge, as shown in Fig. 12. Six units of rapid release system were applied for loading. After getting the effective loading points, it was determined to place them at both mountain and seaside piers between P462 and P464. Loading positions and measured items as well as positions of measurement are also shown in Fig. 12.

4.2. Static loading test

Static loading test was carried out for the piers of both mountain and seaside individually or altogether between P462 and P464. Further, simultaneous loading test was carried out on three bridge piers. The load was gradually increased in the order of 50, 100, 150, and 180 tf. As an example of the result of static loading, deformation of pier P463 is shown in Fig. 13(a) and (b) when piers between P462 and P464 were loaded on the mountain side only and simultaneously from both sea and mountain sides.

As seen from this figure, the loading on one pier represents bigger deflection of loaded pier while the other members show practically less deflection. Also the case of simultaneous loading from sea and mountain side piers confirms the move to lateral direction but even in this case the deflection value of the upper part is smaller than the lower one. Deflection form of the whole bridge in lateral direction at this time is shown in Fig. 14.

The maximum deflection is 110 mm at the pier P463 with the load of 180 tf while there was little deflection on the pier with no loads. Fig. 15 shows the relationship between the horizontal spring rigidity and deflection obtained in the laboratory test as well as the actual test on bridges. There is a slight difference within a small deflection but the actual data of the horizontal spring rigidity remain the same as those done in the laboratory in the range above 80 mm.

4.3. Rapid release test

Rapid release test was carried out, in which the load was reached up to 180 tf and then abruptly released. Deflection and acceleration are shown in Fig. 16 using an example of mountain side P463. Deflection went

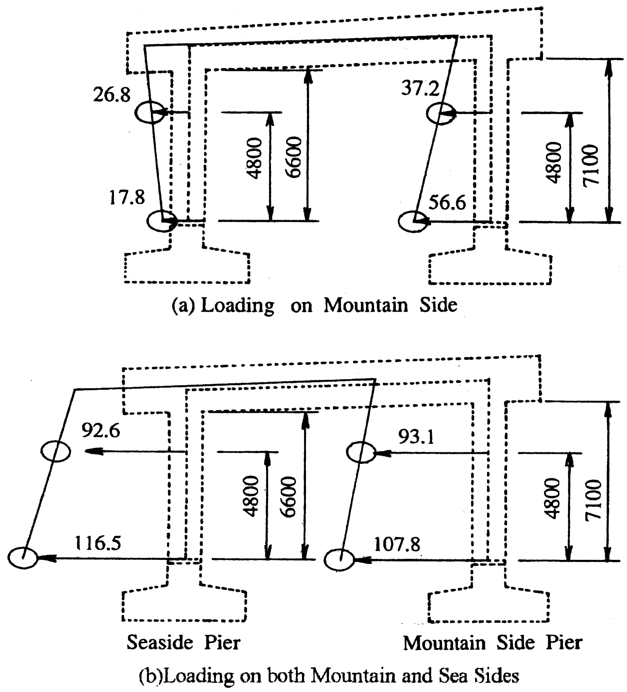

Fig. 13. Deformation of piers.

back near to the original position when load was discharged and the vibration component is damped to diminish. Thereafter the deflection had slowly decreased and in a few minutes after the release went back to the original position completely.

In the response of acceleration, while the free damping vibration is confirmed to remain as in the case of deflection, its vibrated element shows high spectrum at the point of 2 Hz. By measuring rotating deflection of bearing and pursuing the vibrating mode of gate bridge pier, it became apparent that horizontal vibration at the pier foundation had been damped immediately after the release and thereafter rocking vibration was seen at

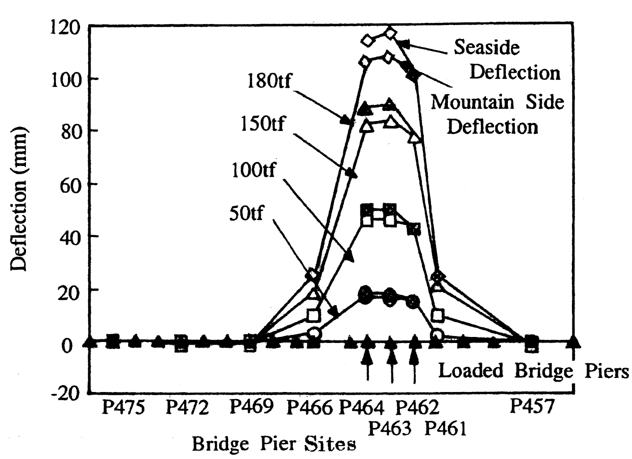

Fig. 14. Deflection of pier loaded on downside.

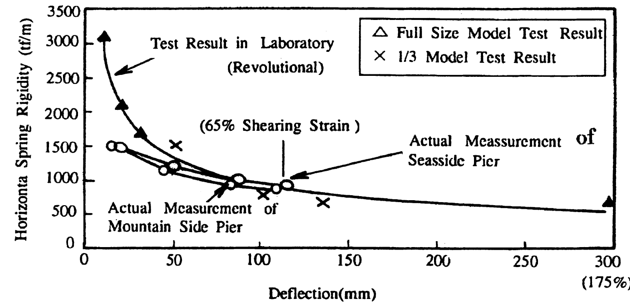

Fig. 15. Design and measurement of spring rigidity.

the center of each bearing. From such observation in the response of the acceleration, higher frequency of vibration is considered to be due to the rocking effect and it corresponds with the result of inherent value analysis of

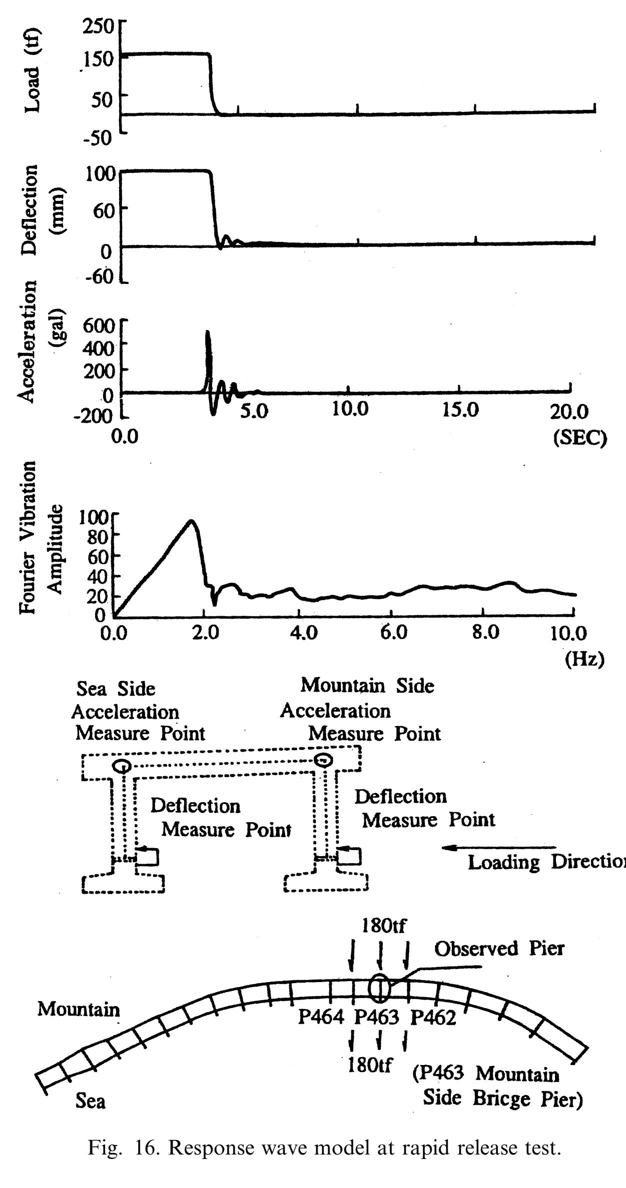

Fig. 16. Response wave model at rapid release test.

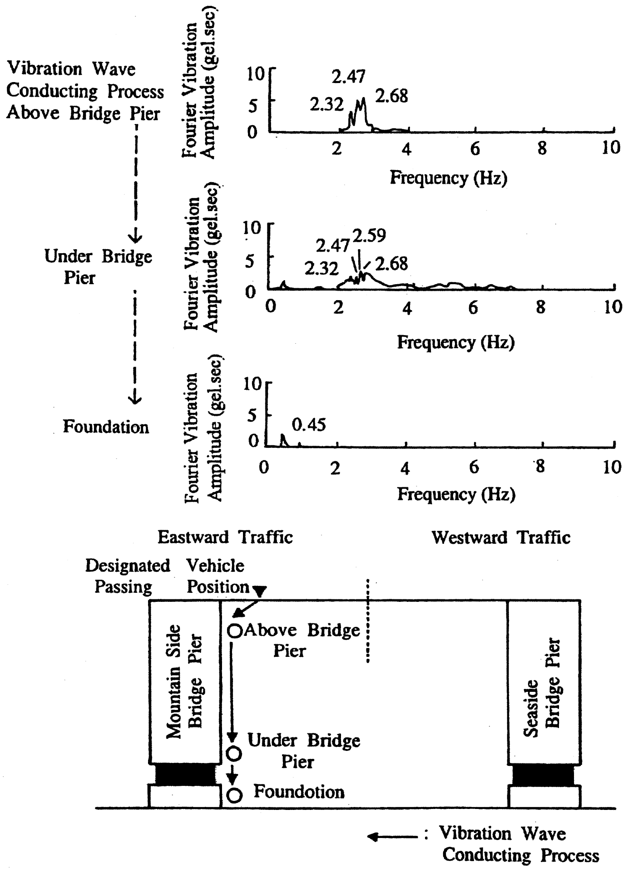

Fig. 17. Damping effect of wave frequency zone at the time of test vehicle running experiment (axial direction).

hinge reaction which substitutes the bearing applied to the plane model.

In the time history response analysis applied on the three-dimensional model that evaluates the rigidity, it is confirmed that vibration modes of 1st through 3rd are all located under 0.7 Hz, while all present experiments under partial vibrating condition show a different vibrating element from the designed vibrating characteristics.

In the design of the upper part, 2% damping was anticipated, however, calculated damping coefficient from the logarithmic decrement of actual damping wave in a vertical direction had dispersed in the 4–5% area.

At the time of rapid release, the representing vibration mode of the main girder and its vibrating frequency varied between 5.3 and 6.3 Hz in the torsional mode, and between 9.0 and 10.0 Hz in the bending mode.

4.4. Vehicle running test

Vehicle load running test had been carried out at the speed of 20, 40, 60 km/h with one vehicle and parallel drive of 2 or 4 vehicles at 20 km/h speed, and the effect of each running pattern was studied. As an example of

Fig. 18. Benten Viaduct (completed).

the result, the pattern for the damping effect taken from the longitudinal direction of bridge with one vehicle at the speed of 60 km/h is shown in Fig. 17.

Both underneath and upper bridge pier vibration had prevailed to show 2.32, 2.47 and 2.66, however, the above frequency zone did not prevail at the foundation. Similar tendency was observed in the lateral direction (Fig. 18).

Acknowledgements

The authors reported the outline of the design as well as installation techniques taken for Benten Viaduct. As a result of these efforts, the viaduct was finally completed and reopened on 17 July 1996. There were many new challenges during the design stage of this innovative structure and in the measures taken for the environment. The authors hope that our experience will be helpful in creating other earthquake-resisting bridges.

References

[1] Hayashi Hidenao, Narita Nobuyuki, Maeda Yukio. Determination method of characteristic values and estimating the plastic deformation of seismic-isolation bridges. In: 3rd Colloquium on Vibration Control of Structures Part B, 1993.

[2] Railway Technical Research institute, Seismic Vibration Report on The Hanshin Awaji Earthquake, 1995 and its analysis, JRVI, I Earthquake Report No. 23c, Nakamura, 1995.

[3] The Ministry of Construction, Guide Specifications for Reconstruction and Repair of Highway Bridges Which Suffered Damage due to the Hyogo-ken Nanbu Earthquake, to New Highway Bridges and Seismic Strengthening.

[4] Hayashi Hidenao, Kawakita Shiro, Hayashida Mitsuhiro. Design and techniques for the 'Benten Viaduct', long-span and high-rise structure, Kobe, 1998.

[5] Hayashi Hidenao, Kawakita Shiro, Nakahigashi Takehiko, Sanada Kenji. Design of the 19-span continuous rigid frame bridge with seismic isolator, New Technologies in Structural Engineering, Lisbon, 1997.